



## Real-Time Gated Proton Therapy: Commissioning and Clinical Workflow for the Hitachi System



Hao Chen (PhD)<sup>1,\*</sup>, Emile Gogineni (DO)<sup>1,2</sup>, Yilin Cao (MD)<sup>1,3</sup>, John Wong (PhD)<sup>1</sup>, Curtiland Deville (MD)<sup>1</sup>, Heng Li (PhD)<sup>1</sup>

<sup>1</sup> The Johns Hopkins University School of Medicine, Baltimore, Maryland, USA

<sup>2</sup> The Ohio State University Medical School, Columbus, Ohio, USA

<sup>3</sup> Dana-Farber/Brigham and Women's Cancer Center, Boston, Massachusetts, USA

### ARTICLE INFO

#### Keywords:

Real-time gated proton therapy  
Motion management for IMPT  
Intrafractional motion management  
Proton therapy for prostate cancer  
Image-guided proton therapy

### ABSTRACT

**Purpose:** To describe the commissioning of real-time gated proton therapy (RGPT) and the establishment of an appropriate clinical workflow for the treatment of patients.

**Materials and Methods:** Hitachi PROBEAT provides pencil beam scanning proton therapy with an advanced onboard imaging system including real-time fluoroscopy. RGPT utilizes a matching score to provide instantaneous system performance feedback and quality control for patient safety. The CIRS Dynamic System combined with a Thorax Phantom or plastic water was utilized to mimic target motion. The OCTAVIUS was utilized to measure end-to-end dosimetric accuracy for a moving target across a range of simulated situations. Using this dosimetric data, the gating threshold was carefully evaluated and selected based on the intended treatment sites and planning techniques. An image-guidance workflow was developed and applied to patient treatment.

**Results:** Dosimetric data demonstrated that proton plan delivery uncertainty could be within 2 mm for a moving target. The dose delivery to a moving target could pass 3%/3 mm gamma analysis following the commissioning process and application of the clinical workflow detailed in this manuscript. A clinical workflow was established and successfully applied to patient treatment utilizing RGPT. Prostate cancer patients with implanted platinum fiducial markers were treated with RGPT. Their target motion and gating signal data were available for intrafraction motion analysis.

**Conclusion:** Real-time gated proton therapy with the Hitachi System has been fully investigated and commissioned for clinical application. RGPT can provide advanced and reliable real-time image guidance to enhance patient safety and inform important treatment planning parameters, such as planning target volume margins and uncertainty parameters for robust plan optimization. RGPT improved the treatment of patients with prostate cancer in situations where intrafraction motion is more than defined tolerance.

### Introduction

Proton therapy has the potential to reduce the dose to normal tissues while maintaining target coverage, compared to conventional X-ray therapy.<sup>1,2</sup> However, the proton dose distribution is susceptible to respiratory motion and anatomic changes throughout the treatment course.<sup>3</sup> Techniques including breath hold and respiratory gating were developed to improve the accuracy of radiation therapy by motion reduction.<sup>4</sup> A prospective study of repository-gated proton beam therapy for liver tumors<sup>5</sup> demonstrated the feasibility of performing gated

proton therapy. However, the proton beam was manually triggered using an external surrogate signal, in addition to the 130 ms latency that was observed in the preclinical study for the same delivery system.<sup>6</sup> The Mayo Clinic has implemented automatically respiratory-gated spot-scanning proton therapy with the real-time position management system (Varian).<sup>7</sup> This active motion management uses an infrared camera to track patient surface motion. The benefit of the real-time gated proton therapy (RGPT) system investigated in this study is that it tracks implanted fiducials placed within or surrounding the tumor, which could therefore be a better surrogate of tumor motion.<sup>8</sup> In

\* Corresponding author.

E-mail addresses: [hchen142@jhu.edu](mailto:hchen142@jhu.edu) (H. Chen), [emile.gogineni@osumc.edu](mailto:emile.gogineni@osumc.edu) (E. Gogineni), [ycao17@bwh.harvard.edu](mailto:ycao17@bwh.harvard.edu) (Y. Cao), [jwong35@jhmi.edu](mailto:jwong35@jhmi.edu) (J. Wong), [cdeville@jhmi.edu](mailto:cdeville@jhmi.edu) (C. Deville), [hengli@jhmi.edu](mailto:hengli@jhmi.edu) (H. Li).

<https://doi.org/10.1016/j.ijpt.2024.01.001>

Received 1 August 2023; Received in revised form 21 January 2024; Accepted 23 January 2024

2331-5180/© 2024 Published by Elsevier B.V. on behalf of Particle Therapy Co-operative Group. This is an open access article under the CC BY-NC-ND license (<http://creativecommons.org/licenses/by-nc-nd/4.0/>).

addition, the gated signal from RGPT is connected to the delivery system, so the proton beam can be triggered automatically according to the gating signal with minimum latency. Hitachi has previously published details of the RGPT system design.<sup>9</sup> This study describes the commissioning and clinical workflow of the RGPT system for the Hitachi PROBEAT system.

#### Real-time gated proton therapy for Hitachi system

Leveraging its advanced imaging system, the Hitachi PROBEAT is capable of RGPT, which can turn off the proton beam if a target is outside a predefined area, allowing for high-quality treatment delivery. In this section, we will introduce the imaging system, beam control mechanism, and software for Hitachi RGPT.

#### Image system and properties in the gantry

Each gantry has 2 large orthogonal fixed digital flat panel detectors (FPDs), called xRay1 and xRay2, which are 45 degrees away from the proton beam direction on both sides. The distance from the x-ray source and FPD to the isocenter is 1.55 m and 0.6 m, respectively. Each FPD provides a maximum resolution of  $1024 \times 1024$  pixels with 0.417 mm pixel size equivalent to 0.3 mm at the isocenter. The fluoroscopy-based RGPT imaging software provides a fixed  $20 \text{ cm} \times 20 \text{ cm}$  field of view (FOV) for both FPDs with pulse rate options of 1, 7.5, 15, or 30 frames per second. The recorded image is  $720 \times 720$  pixels per frame at 30 FPS. The 3-dimensional spatial recognition accuracy off-isocenter is within 1 mm for the fluoroscopy image mode. The 2 mm motion tracking accuracy is approximately 6.7 pixels in the image.

#### Proton beam control and gating signal

The Hitachi system controls the proton beam through acceleration, extraction, and deceleration, which takes roughly 1, 5, and 0.65 seconds, respectively. The beam is only turned on during the extraction phase when the gate signal is on. Figure 1 demonstrates how these aspects are related to one another. The Hitachi system will automatically stop the current treatment when the gating signal is off for more than a predefined period of time.

Both FPDs, the 2 ion chambers for dose monitoring, and the proton beam nozzle are all within close proximity to one another. Therefore, the proton beam is turned off during fluoroscopy imaging to avoid issues with MU miscounting. The maximum latency between the gating signal and the proton beam control signal is  $< 0.1$  seconds. The “Beam on Gate” curve of Figure 1 shows that the beam is on for about 0.4 seconds approximately every 3 seconds. The maximum latency should be also considered to ensure high-quality plan delivery of the

RGPT plan. With 0.1 seconds maximum latency, the delivery uncertainty accuracy for the motion target should be achievable within 2 mm with the proper commissioning and clinical workflow.

#### Parameters for real-time gated proton therapy

The fluoroscopy images taken with both FPDs are transferred to the RGPT control server and image recorder server through 2 high-performance video splitters. The RGPT control server provides a software GUI for the radiation therapist(s) to monitor and operate the RGPT function, which tracks the target position in real-time. The image recorder server stores all fluoroscopy images for off-line reviewing. The software graphical user interface (GUI) shows the important RGPT parameters: gating signal, matching score, and gating tolerance with other adjustable parameters for the fluoroscopic imaging, including kV, mA, ms, pulse rate, collimator size, fluoro timer, and accumulated timer.

Hitachi PROBEAT RGPT uses a gating signal to turn the beam on or off and matching score (a value between 1 and 99) to evaluate and preempt potential delivery issues. A lower matching score means that the RGPT system is less confident about the current target tracker result. The matching score depends on many factors, such as template quality, the current fluoroscopy signal quality, the tracking target’s motion velocity, and scatter/noise from the collimator edge. The matching score can be improved through the following adjustments:

- Increasing the pulse rate to reduce motion between 2 sequential fluoroscopy images
- Selecting the proper tracking target inside soft tissue
- Increasing kV, mA, and/or ms to improve signal quality.

The contrast ratio of signal between the tracked target to the background from FPDs may be changed when following target motion, especially for targets close to the diaphragm. The patient’s image dose exposure and plan delivery efficiency should be also carefully considered during the adjustment of imaging parameters. A set of 2 matching score thresholds can be defined in the RGPT software. Real-time gated proton therapy will

- Immediately pause the proton beam when either matching score is below the lower threshold.
- Enter a warning status with a gating signal on when either matching score is between 2 thresholds. The gating signal will be off when the warning status keeps on for a customizable period of time (eg, several seconds).
- Keep the gating signal on when both matching scores are larger than the higher threshold.

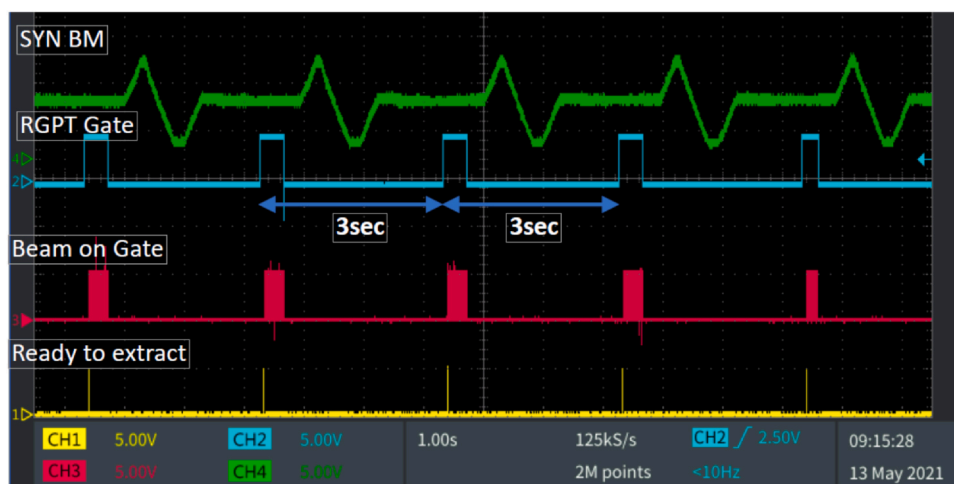


Figure 1. RGPT control signaling, as it relates to (1) the proton beam phase of the synchrotron (“SYN BM”), (2) the RGPT gating signal (“RGPT Gate”), and (3) the beam current gating at isocenter (“Beam on Gate”). Abbreviation: RGPT, real-time gated proton therapy.

The maximum tolerance for target motion should be individually defined in 3 directions and depend on the tumor site, setup protocol, and plan technique. The maximum tolerance values should be verified with dosimetry and end-to-end testing. The gating signal is turned off when the tracked target is outside of tolerance in any direction.

**Methods and materials**

The Hitachi system provides sufficient safety interlock for RGPT to ensure proton plan delivery quality. In this section, we describe a comprehensive quality evaluation including end-to-end dosimetry evaluation to commission the RGPT function for patient treatment. Prior to RGPT commissioning, we performed routine QA for image quality and image dose, but these regular processes will not be detailed in this section.

*Equipment, plan, and setup*

The CIRS Dynamic System (SUN NUCLEAR, Melbourne, FL) combined with RSD Anthropomorphic Thorax Phantom (Radiology Support Devices, Inc, Long Beach, CA) or CIRS plastic water was used to mimic target motion. The OCTAVIUS 1500XDR (PTW, Freiburg, Germany) was utilized to measure end-to-end dosimetry accuracy. The OCTAVIUS is located at the top of the CIRS Dynamic System with sufficient buildup. The Civco Fiducial Marker (Medtec LLC, Coralville, Iowa) was used as the tracking target. The fiducial marker was outside of the field to avoid interfering with the measurement result. A plan for a 10 cm cubic target was optimized in Raystation 10. A (Raysearch Laboratories, Stockholm, Sweden). The center of the target is 15 cm from the surface. The MU/Spot was identical in each energy layer. The IMPT plan was delivered through the MOSAIQ oncology information system (Elekta, Stockholm, Sweden) with gating support. The plan setup followed our routine clinical workflow for proton plans.

*Real-time gated proton therapy plan delivery and measurement*

The orthogonal KV images were used to align the CIRS Dynamic System, OCTAVIUS, and plastic water after setup. We then switched to Hitachi’s RGPT image software called RGPT64, and an initial fluoroscopy image was taken and used to verify the fiducial marker positioning.

The plan was then delivered with several different motion settings using the CIRS Dynamic System, as detailed in Table. OCTAVIUS collected all delivery plan doses with these motion settings at the plan isocenter. The first set of data was collected without motion. The motion direction was the same as the proton pencil beam scanning direction. Under this motion direction setup, the motion would have a maximum dosimetric impact.

**Table**  
Motion setting for end-to-end test and related plan delivery time with RGPT.

Simulation No.	Cycle (s)	Motion Amp ( ± mm)	Gating tolerance ( ± mm)	Gate position	Delivery time (min)
1	Static	NA	2	NA	1
2	6	5	3	Zero-cross	4
3	6	10	3	Zero-cross	7
4	6	15	3	Zero-cross	12
5	6	20	3	Zero-cross	19
6	6	5	2	Zero-cross	5
7	6	10	2	Zero-cross	12
8	6	15	2	Zero-cross	22
9	5	15	2	Zero-cross	22
10	6	10	2.5	Summit	4
11	6	15	2.5	Summit	5
12	6	20	2.5	Summit	7

**Abbreviation:** RGPT, real-time gated proton therapy.

*Real-time gated proton therapy parameter evaluation*

The minimum fluoroscopy image FOV was 5 cm × 5 cm. The image FOV was minimized to reduce imaging dose while the fiducial motion was not expected to exit this FOV. Both X-ray tubes used the same kV and mA, as dictated by the tumor site. The ms value was always set to 3. Setting a high pulse rate could reduce the fiducial’s absolute motion between 2 sequential fluoroscopy images, and thereby improve matching scores. However, the proton beam pauses during fluoroscopy imaging. The Hitachi system required about 2 seconds from deceleration to the next extraction of the proton beam. Therefore, improper pulse rate settings could cause significantly added time to beam delivery. For our end-to-end testing, a pulse rate of 7.5 frames per second was used.

**Results**

Real-time gated proton therapy can deliver treatment to a moving target with less uncertainty but comes at the cost of greater beam delivery time per field. We evaluated the RGPT function with the perspective of 2 major concerns: plan delivery efficiency and plan delivery uncertainty. The same plan was delivered with different motion setups, as detailed in Table. The motion pattern was a sine wave with different amplitudes and cycles. The fiducial marker in the template could be selected at either of 2 positions of the sine curve: zero-cross (middle line) and summit (crest or trough). The fiducial marker velocity would reach maximum at zero-cross position and minimum at summit position. The measurements obtained without motion were used as a reference for this evaluation.

*Plan delivery efficiency*

In the absence of simulated motion, the estimated fiducial marker position in fluoroscopy imaging was always within the 2mm gating tolerance. The plan was delivered in under 1 minute including all fluoroscopic imaging time, and therefore we used 1 minute (T<sub>base</sub>) as the baseline reference for plan delivery efficiency. The last column of Table lists the delivery time for the various motion settings and gating tolerances. In theory, the plan delivery efficiency would be primarily dictated by the gating tolerance and motion amplitude. The total delivery time would thus be

$$T_{total} = T_{base} * M_{amp}/G_{tol} + T_{image}$$

Here, M<sub>amp</sub>, G<sub>tol</sub>, and T<sub>image</sub> are motion amplitude, gating tolerance, and total time for fluoroscopic imaging, respectively. T<sub>image</sub> was relatively small compared with T<sub>base</sub> and could be ignored in most situations. Based on simulations 10 to 12, the total delivery times increased

to 4, 5, and 7 minutes (from the 1 minute baseline) when  $M_{\text{amp}}/G_{\text{tol}}$  were 4, 6, and 8, respectively, where the additional time for simulations 11 and 12 was from fluoroscopy.

When we used the fiducial marker position at zero-cross as a reference, the total plan delivery time did not linearly increase with motion amplitude. Based on simulations 2 to 5, the delivery times increased to 4, 7, 12, and up to 19 minutes when  $M_{\text{amp}}/G_{\text{tol}}$  were 1.7, 3.3, 5.0, and 6.7, respectively. The plan delivery efficiency was dramatically reduced in a nonlinear fashion due to 3 factors:

1. The fiducial marker's velocity reached its maximum at the zero-cross position. The time window for the gating-on signal was relatively short compared with the reference at the summit. The latency of the gating signal (maximum up to 0.1 seconds) impacted delivery efficiency more significantly when each motion cycle had the shorter absolute beam on time. The ratio of delivery time to motion amplitude increased for simulation 5 compared with that from simulation 2.
2. When the fiducial marker's velocity reached its maximum at the zero-cross position, the positional discrepancy between 2 sequential fluoroscopic images was also maximized. This caused the RGPT system to track the target with the lower matching score which could temporarily halt treatment delivery, causing an increase in total delivery time.
3. When the reference point was set at the zero-cross with a 6-second motion cycle, the beam-off time between 2 sequential beam-on points was equal to  $(T_{\text{cycle}} - T_{\text{on}})/2$ , that is, half the value of the beam-off time for a summit reference point. The Hitachi system required about 2 seconds between deceleration to the next extraction of the proton beam. When beam-off was close to or less than 2 seconds, the system simply would not be ready to extract and deliver the proton beam even when the gating signal was on. Under this situation, the Hitachi system skipped the current beam-on period and waited for the next gating-on signal.

The same plan delivery efficiency trend was seen for simulations 6 to 9 in Table. Based on these simulations, plan delivery efficiency could be maximized when the fiducial marker reference position was selected at the motion summit to account for the fiducial marker motion velocity and the time required for the phases of Hitachi beam delivery.

#### Dosimetry result with motion phantom

The dosimetry result of simulation 1 was used as the reference for comparison. To maintain consistency with our clinical robust optimization planning protocol, we used  $\pm 2$  mm for gating tolerance for the dosimetry results in this section. The motion cycle was 6 seconds. The 3%/3 mm gamma analysis with the action levels of 90% was used for data analysis.

When the amplitude of motion was  $< 2$  cm ( $\pm 1$  cm), the Hitachi system could uniformly deliver the plan with 2 mm uncertainty independent of the reference position (cross-zeros or summit position), as shown in Figure 2A and D. Motion in the vertical direction produced nonflat isodose lines at both the top and bottom because the motion and proton beam scanning were in the same direction and nonsynchronized. Figure 2D shows that the dosimetry result was acceptable for patient treatment in both (1) the dose profile in the motion direction, and (2) gamma analysis results.

When the motion amplitude increased up to 3 cm ( $\pm 1.5$  cm) or even 4 cm ( $\pm 2$  cm), the Hitachi system was unable to deliver a uniform dose to the target at a gating tolerance of 2 mm with the reference position at cross zero. Figure 2B and C shows large discrepancy areas inside the target. Both the dose profile and gamma analysis confirmed

that the final delivered dose was not acceptable for patient treatment. The gamma analysis pass rate was  $< 90\%$ .

The fiducial marker reference position was critical for plan delivery accuracy with RGPT. For the same motion amplitude, that is, up to 4 cm ( $\pm 2$  cm), the Hitachi system could successfully deliver a uniform dose to the target when the reference position was selected at cross zero (as demonstrated in Figure 2D).

Figure 2E replicates the motion settings of Figure 2D ( $\pm 2$  cm), but demonstrates the dosimetry in the absence of RGPT. As expected, significant underdosing occurred at the summit and valley of motion. This supports that RGPT with the Hitachi system improved and may bring plan delivery to an acceptable quality level for patient treatment even when movement is up to 4 cm.

#### Discussion: real-time gated proton therapy clinical application and workflow

The prospective study shows that RGPT for prostate cancer was as safe as conventional proton beam therapy.<sup>10</sup> In this section, we will use prostate radiotherapy cases to demonstrate the design, optimization, and delivery of clinical treatment plans with RGPT.

#### Fiducial marker

A larger fiducial marker can improve the matching score in the Hitachi RGPT system. However, the tradeoff is that larger fiducial markers may require larger needles to implant them and will also introduce more artifacts in CT/CBCT (computed tomography/cone-beam computed tomography) images. The proper fiducial marker size should therefore be selected after systematic evaluation. The VISICOIL 0.5 mm  $\times$  5 mm or 0.75 mm  $\times$  5 mm titanium fiducial markers were found to be most appropriate for prostate RGPT following our investigation. Figure 3 shows that the matching score nonlinearly decreased while water equivalent thickness (WET) increased. The larger fiducial marker had a higher matching score under the same WET (Figure 3).

In some instances, multiple fiducial markers might be implanted closely inside the target. The isocenter of the proton plan was set close to the fiducial marker to minimize the fluoroscopy imaging dose with a small FOV (Figure 4). After all the beam directions intended for use in the plan were determined and the fiducial markers were contoured, the digitally reconstructed radiograph for each treatment field was generated from both imaging panels, as shown in Figure 5. A single best fiducial marker for tracking was selected with the following considerations:

- The fiducial marker should be closest to the isocenter in the majority of digitally reconstructed radiograph images.
- The fiducial marker should have better optimal image contrast from the background, usually against a soft tissue background. Bone and metal impacts in the background should be avoided.

#### Real-time gated proton therapy protocol setup

The clinical RGPT protocol for each tumor site should be evaluated and set up based on plan delivery efficiency and plan delivery dosimetry accuracy. The parameters of RGPT, informed by end-to-end evaluation, should be adjusted to achieve the best system performance. In this section, we review an RGPT protocol setup with prostate cancer treatment as an example.

1. Fluoroscopic image quality for fiducial marker  
Automatic fiducial marker tracking demands high signal-to-

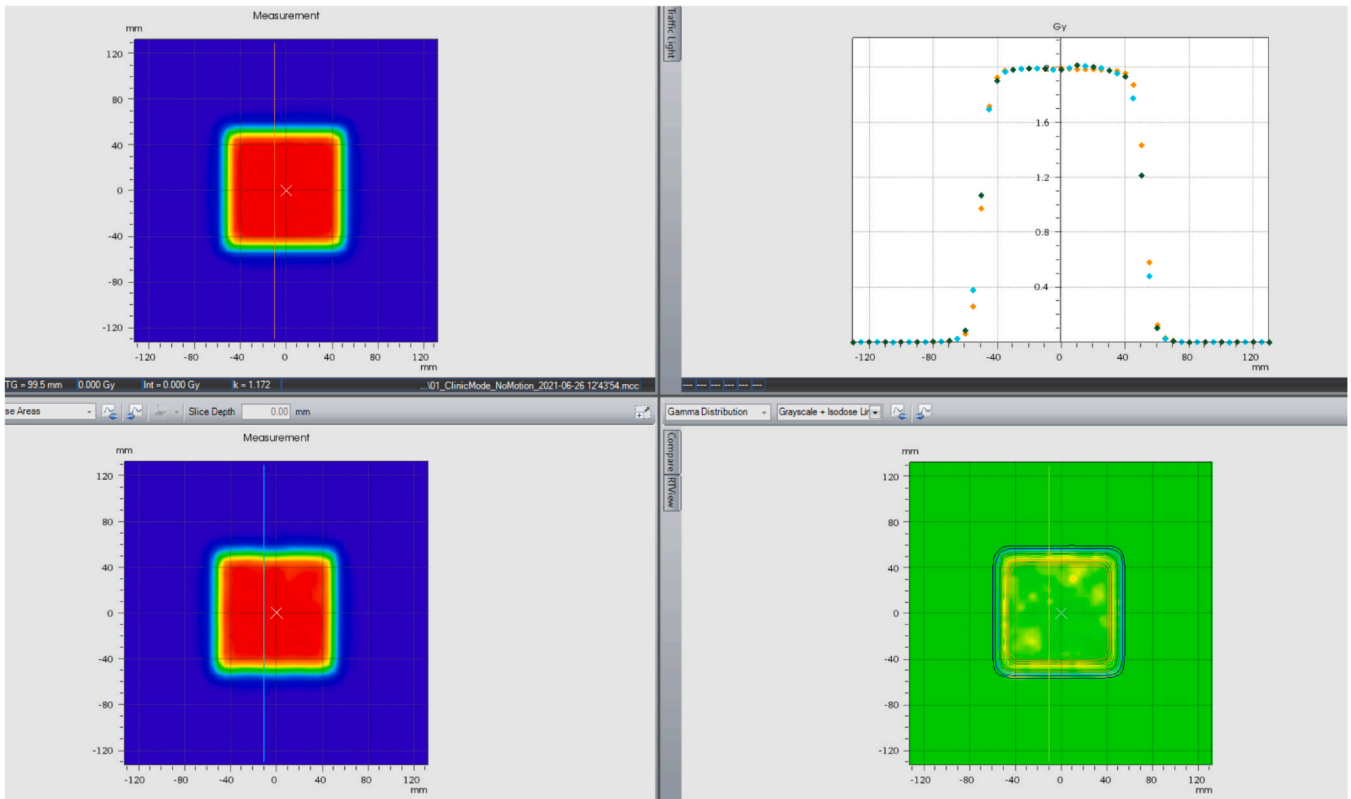


**Figure 2.** (A) The top left: dosimetry measurement without motion. The bottom left: dosimetry measurement (real-time gated proton therapy [RGPT]) with  $\pm 1$  cm motion in 6 seconds while the reference at cross-zero position. The top right: profile comparison in motion direction. The bottom right: gamma analysis. (B) The top left: dosimetry measurement without motion. The bottom left: dosimetry measurement (RGPT) with  $\pm 1.5$  cm motion in 6 seconds while the reference at cross-zero position. The top right: profile comparison in motion direction. The bottom right: gamma analysis. (C) The top left: dosimetry measurement without motion. The bottom left: dosimetry measurement (RGPT) with  $\pm 2$  cm motion in 6 seconds cycle while the reference is at cross-zero position. The top right: profile comparison in the motion direction. The bottom right: gamma analysis. (D) The top left: dosimetry measurement without motion. The bottom left: dosimetry measurement (RGPT) with  $\pm 2$  cm motion in 6 seconds cycle while the reference is at summit position. The top right: profile comparison in the motion direction. The bottom right: gamma analysis. (E) The top left: dosimetry measurement (RGPT) while  $\pm 2$  cm motion in 6 seconds while the reference at summit position. The bottom left: dosimetry measurement without RGPT. The top right: profile comparison in the motion direction. The bottom right: gamma analysis.

background contrast. With limited fluoroscopy imaging time, it is challenging to identify the fiducial marker inside the prostate, where thickness and density are relatively large or high compared with other tumor sites (eg, lung). All fluoroscopic parameters except sample rate should be defined and evaluated using a phantom with similar WET as the prostate case. Notably, the image panel and calibration are not identical for each proton system. Therefore, the proper parameters should be selected based on phantom evaluation. It is also recommended to create a written protocol with instructions for the radiation therapists. With those instructions, they could adjust the parameters to match the template image created during a simple simulation.

## 2. Pulse rate

The fluoroscopy effective doses ranged between 0.04 and 0.14 mSv/1000 pulses.<sup>11</sup> A low pulse rate of fluoroscopic imaging is recommended to minimize image dose and improve plan delivery efficiency. The pulse rate should be maintained at an adequate level for the automatically matching algorithm of RGPT to track motion with its limited search windows. Based on our end-to-end testing, the pulse rate of 1 per second is adequate for prostate treatment. The effective image dose of 1 fraction prostate treatment would range from 0.0048 to 0.0168 mSv. Meanwhile, a pulse rate of 7.5 is recommended for a moving target. A pulse rate of more than 7.5 is not

recommended when we consider field delivery efficiency.

## 3. Gating tolerance

The tumor target positional uncertainty is not identical across tumor sites or in each dimension. For example, the prostate has more positional variance in the superior and inferior direction due to daily bladder and rectum volume changes. For a moving target, the specific pattern of motion in each direction is not uniform either, such as a lung tumor at the apex versus near the diaphragm. The gating tolerance for RGPT function should be set up individually in 3 directions: superior-inferior, left-right, and anterior-posterior. To properly determine gating tolerance, patient setup uncertainty should be estimated based on existing patient daily setup data for the clinic and disease site. We should also consider the proton plan technique to finalize the gating tolerance. Ultimately, the expected intrafraction motion of the target is most important when choosing gating tolerances, as fiducial markers are typically always aligned to plan position before each individual field.

### Proton planning and patient setup with real-time gated proton therapy

Proton planning technique for RGPT should be adapted according to the results of end-to-end dosimetry. With 2 mm dosimetry delivery uncertainty for a moving target, the setup uncertainty for robust plan

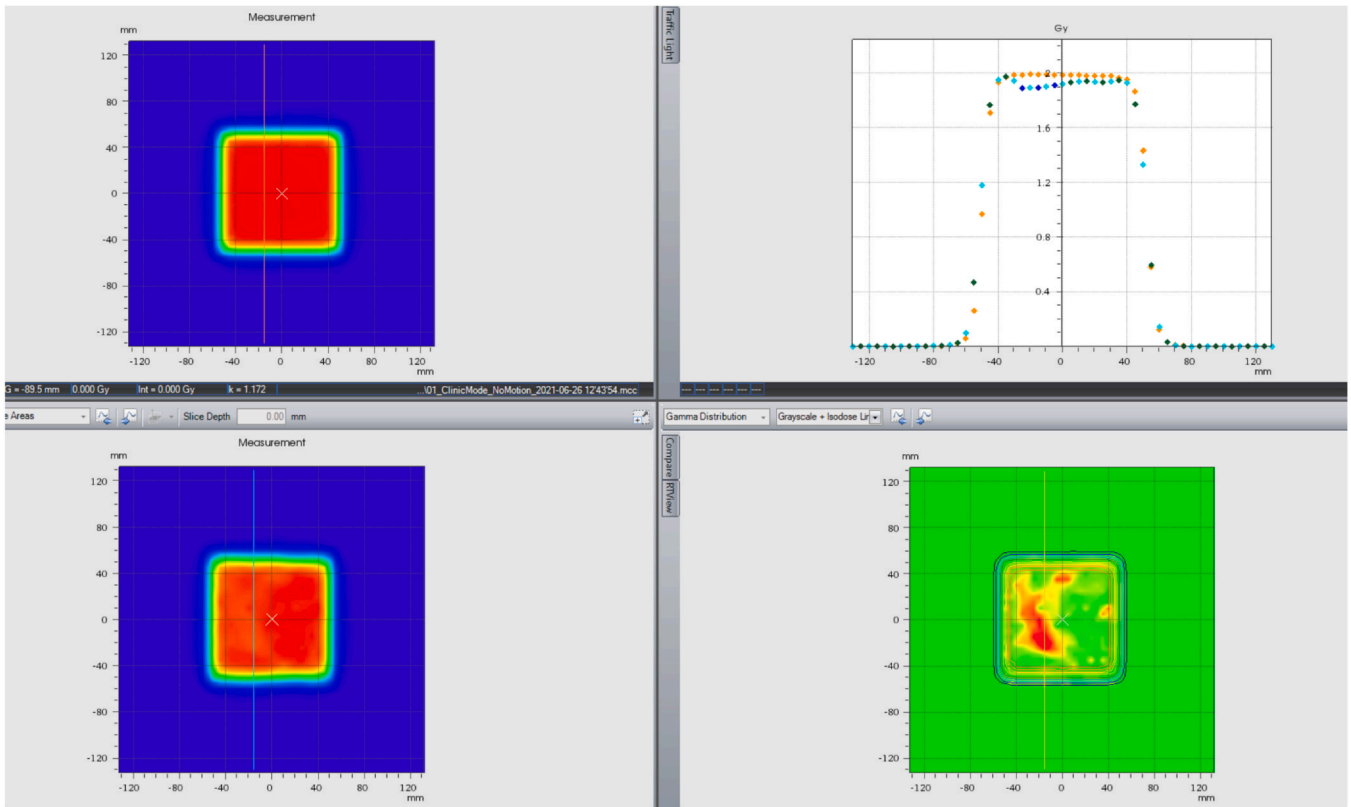


Figure 2. (continued)

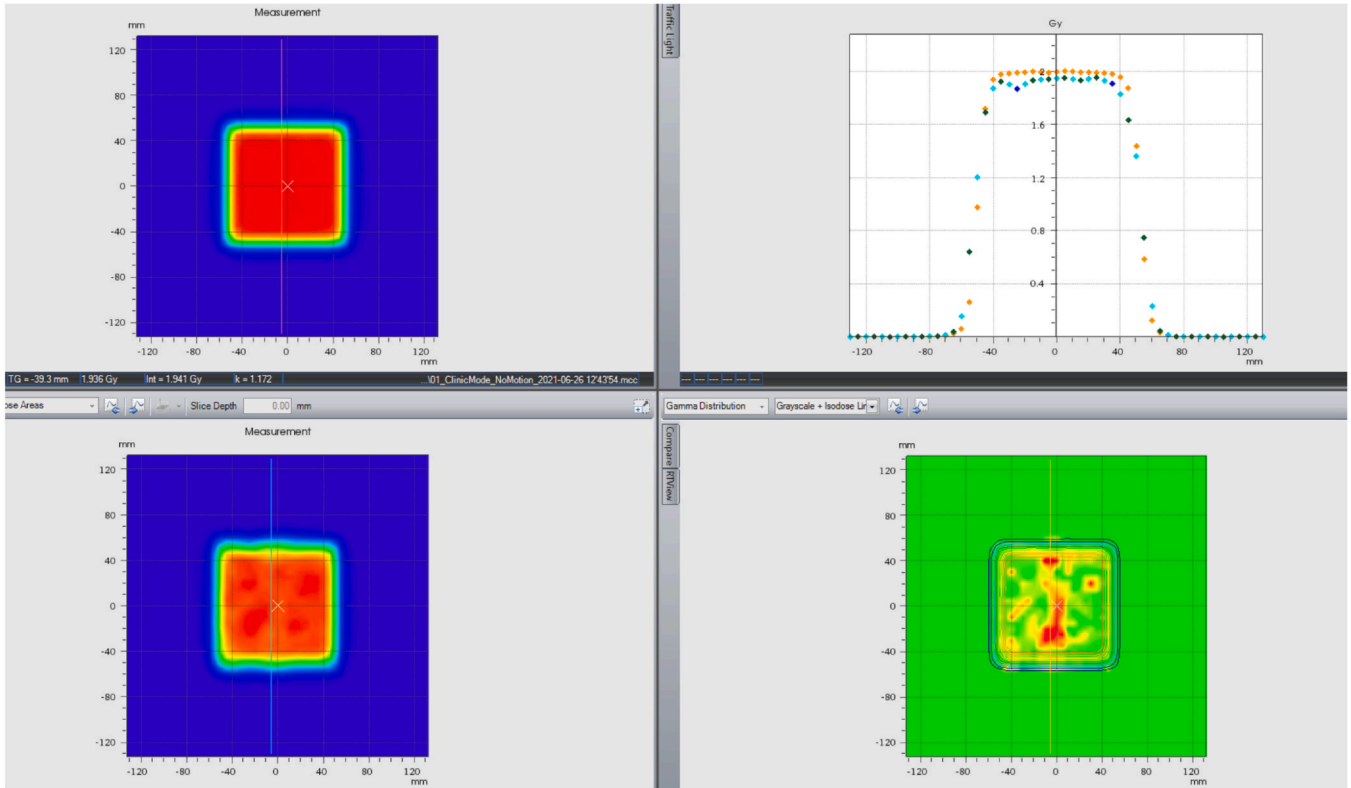


Figure 2. (continued)

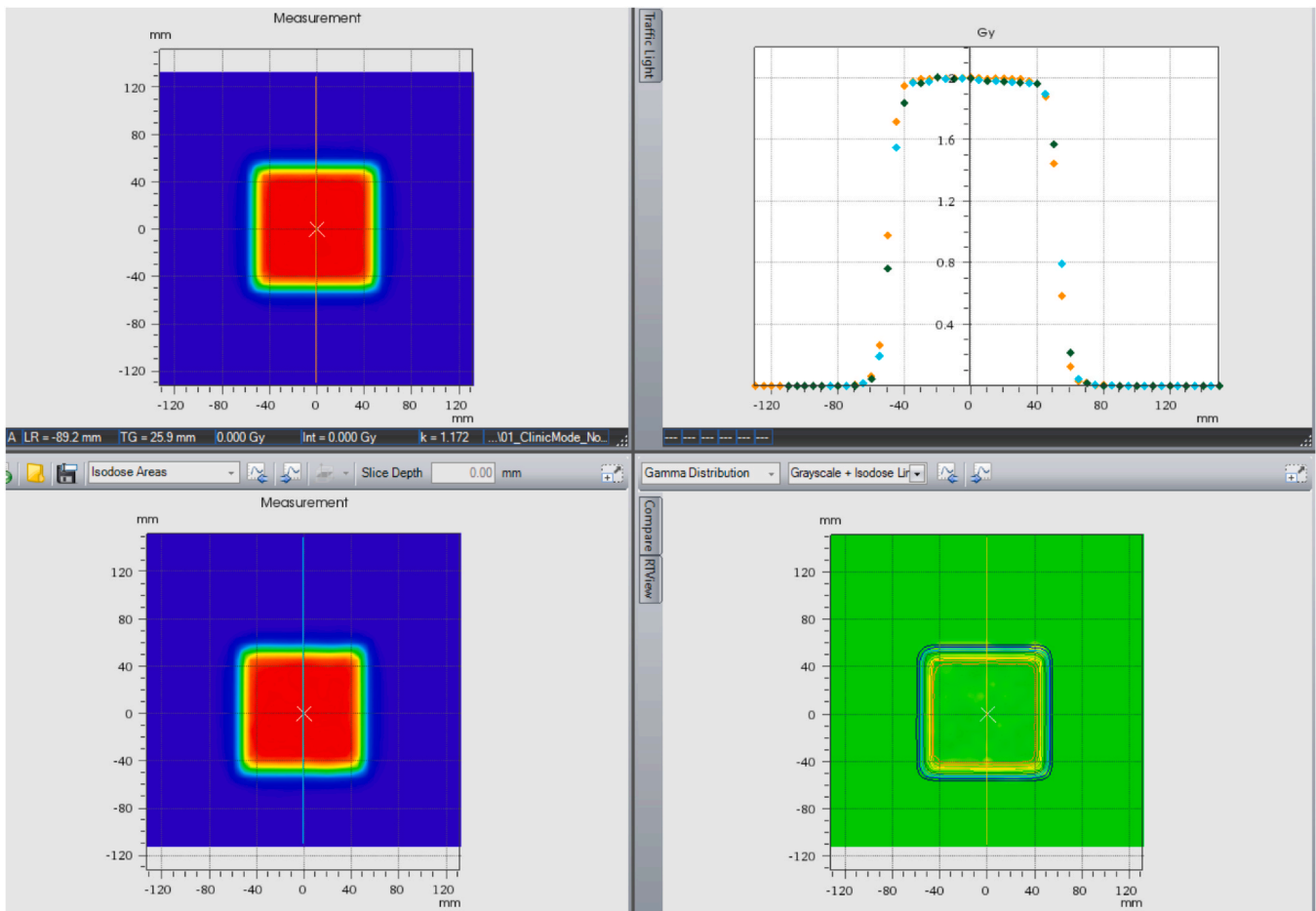


Figure 2. (continued)

optimization and robust plan evaluation could be reduced to 3 mm for most targets. Additional margin could be given for cases demonstrating atypical motion.

The intrafraction motion of the prostate during treatment is limited in most situations. No changes are made to our proton planning technique for prostate plans when utilizing RGPT. After the patient is set up with the normal workflow based on the fiducial marker, we switch to RGPT software and take a quick fluoroscopic image (1-2 frames) to verify the fiducial marker position in the treatment beam’s eye view. The RGPT server will directly communicate with the gantry and proton plan delivery server to gate the entire treatment delivery.

*Fiducial marker template and plan delivery*

Hitachi RGPT system uses a 2D-2D matching algorithm and generates the 2D reference image data for each individual treatment field during simple simulation. The reference image combined with fiducial marker coordinates, which is from the plan structures DICOM file, is used as a fiducial marker template.

After loading the treatment field, a quick fluoroscopic image is taken and is auto-aligned to the template for the current treatment field. The shift between the current fiducial marker and the template is calculated and presented with the matching scores together. The value will be highlighted with a yellow background when out of tolerance and the

safety interlock will be initialized. The positional deviation tolerances are manually set up for each field. The matching score tolerance is defined during system configuration and is identical for all patients. The gating signal will only turn the beam on when the fiducial marker position is within tolerance and the matching scores for both fluoroscopic images are higher than the specified threshold.

The fiducial marker positions and corresponding gating signals are recorded in the proton therapy system log file, which could be utilized to qualitatively analyze treatment.<sup>12-14</sup> Figure 5 shows 3 fiducial marker motion curves in 3 dimensions combined with the corresponding gating signal (black line) during delivery of 3 different treatment fields. In Figure 5A and B, the fiducial marker position was very stable (< 0.5 mm) or shifted minimally (< 1 mm) in all 3 directions throughout the delivery of the entire field, demonstrating typical fiducial marker motion curves during prostate treatment. The fiducial marker intrafraction motion was < 1 mm. However, in Figure 5C, the fiducial marker was observed to have a range of movement of 8 mm in the superior-inferior direction. There was a simultaneous 4 mm range of motion in the anterior-posterior direction. This extreme prostate motion can be caused by situations such as large gas distention within the rectum or an extremely full and unstable bladder during treatment. The proton beam was turned off when the prostate (ie, the fiducial marker) moved outside of tolerance, which allowed for proper treatment of the patient despite the large intrafraction motion.

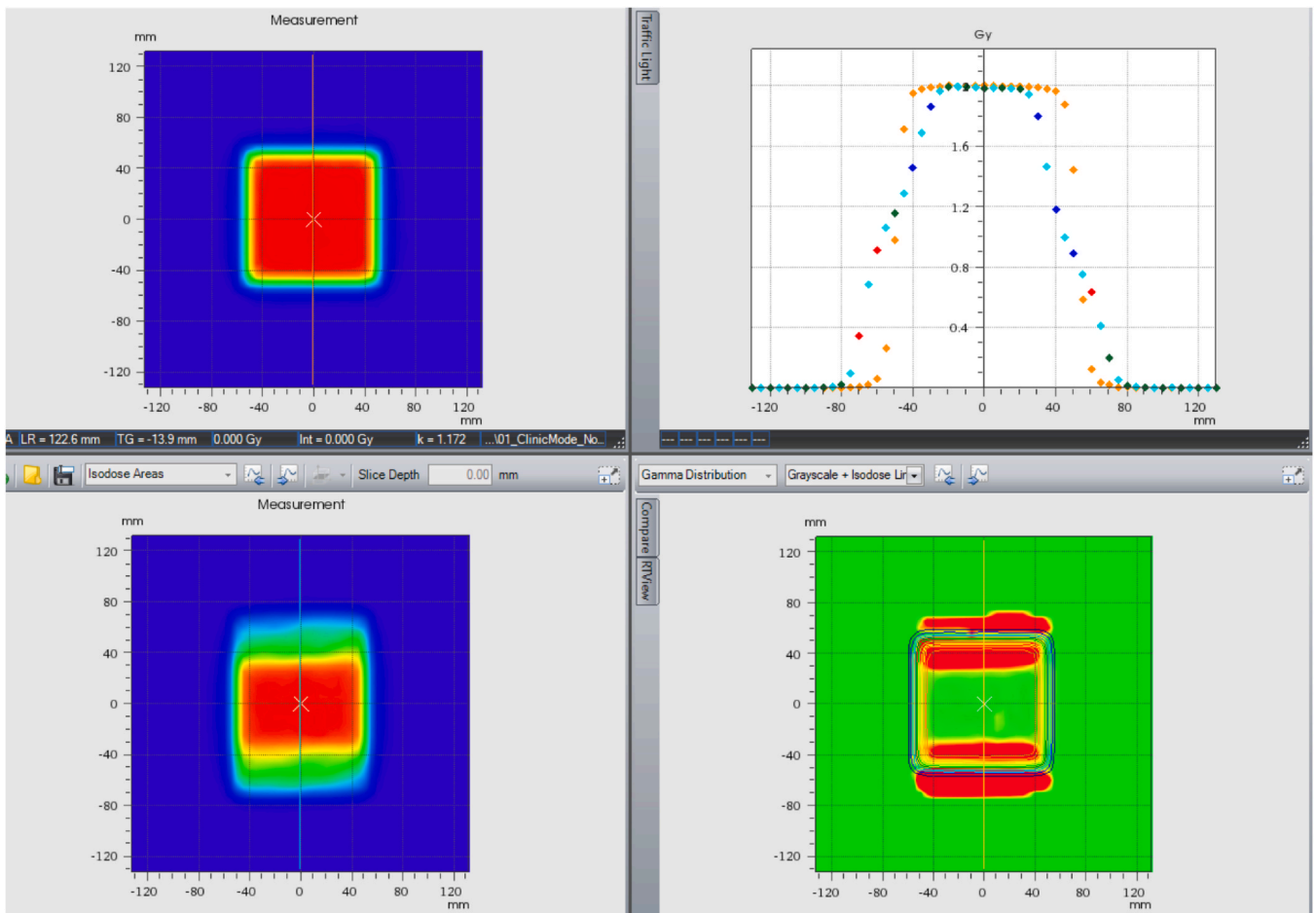


Figure 2. (continued)

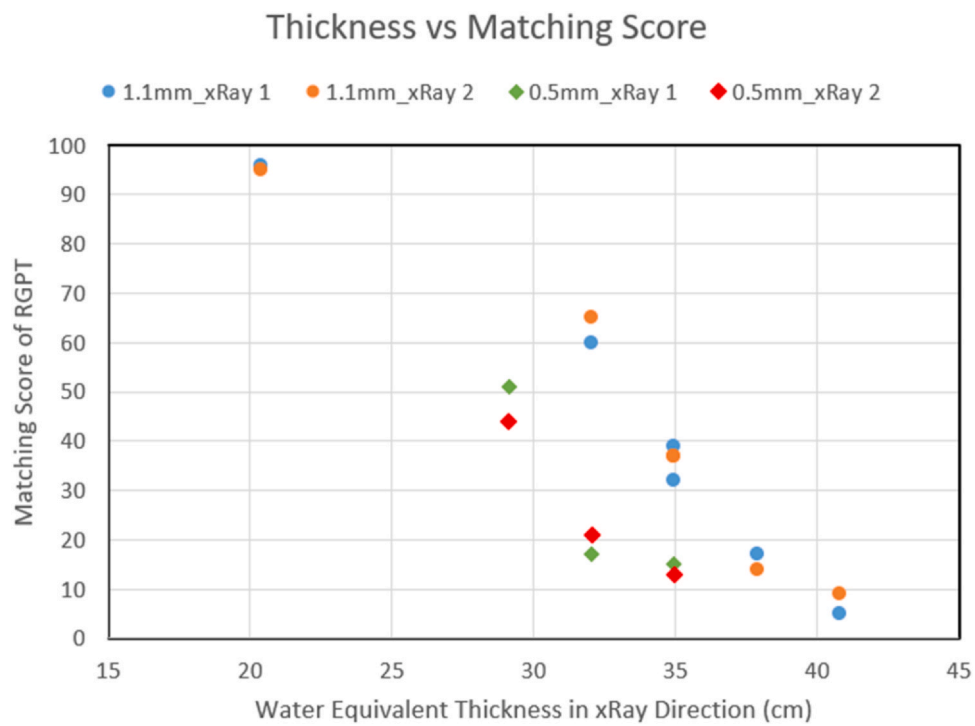
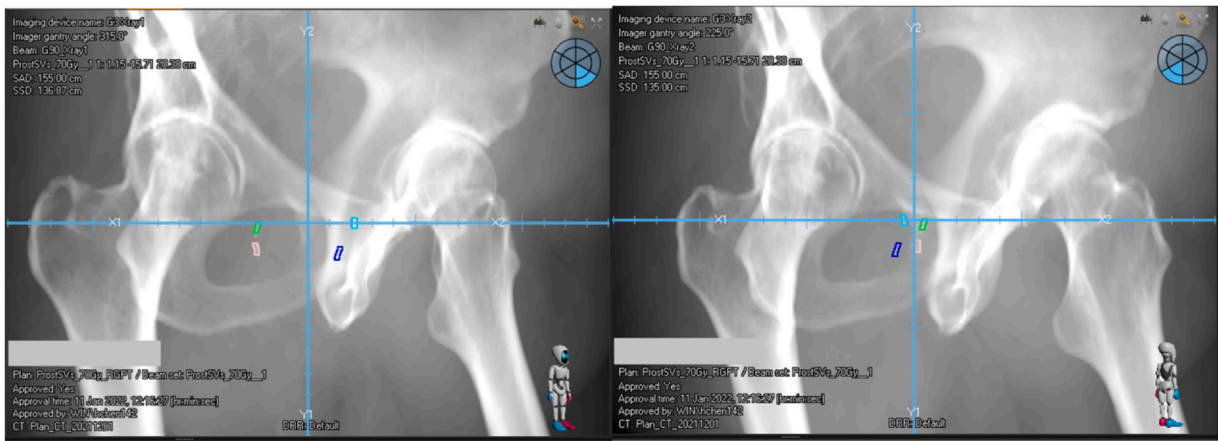
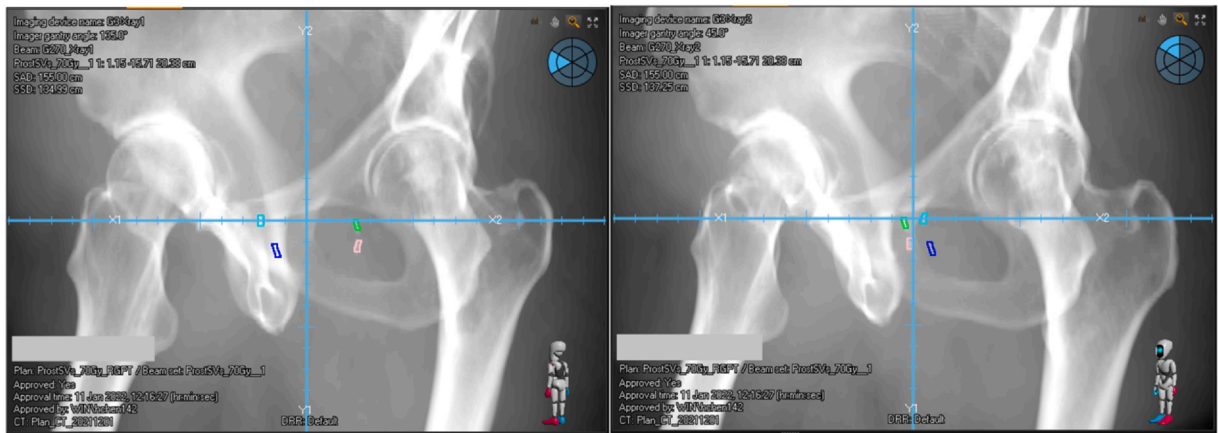


Figure 3. Matching score related to water equivalent thickness in X-ray direction. Abbreviation: RGPT, real-time gated proton therapy.

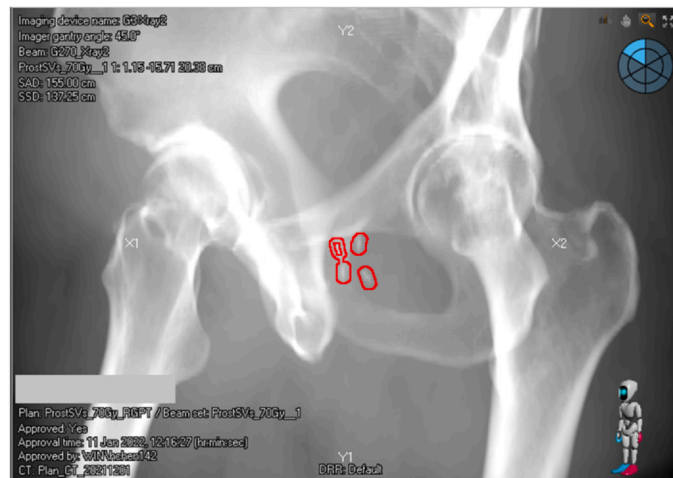




a



b



c

**Figure 4.** (A) DRR for field at 90-degree. (B) DRR for field at 270-degree. (C) Selected Fiducial marker contour for RGPT with 2 mm tolerance. Abbreviations: DRR, digitally reconstructed radiograph; RGPT, real-time gated proton therapy.

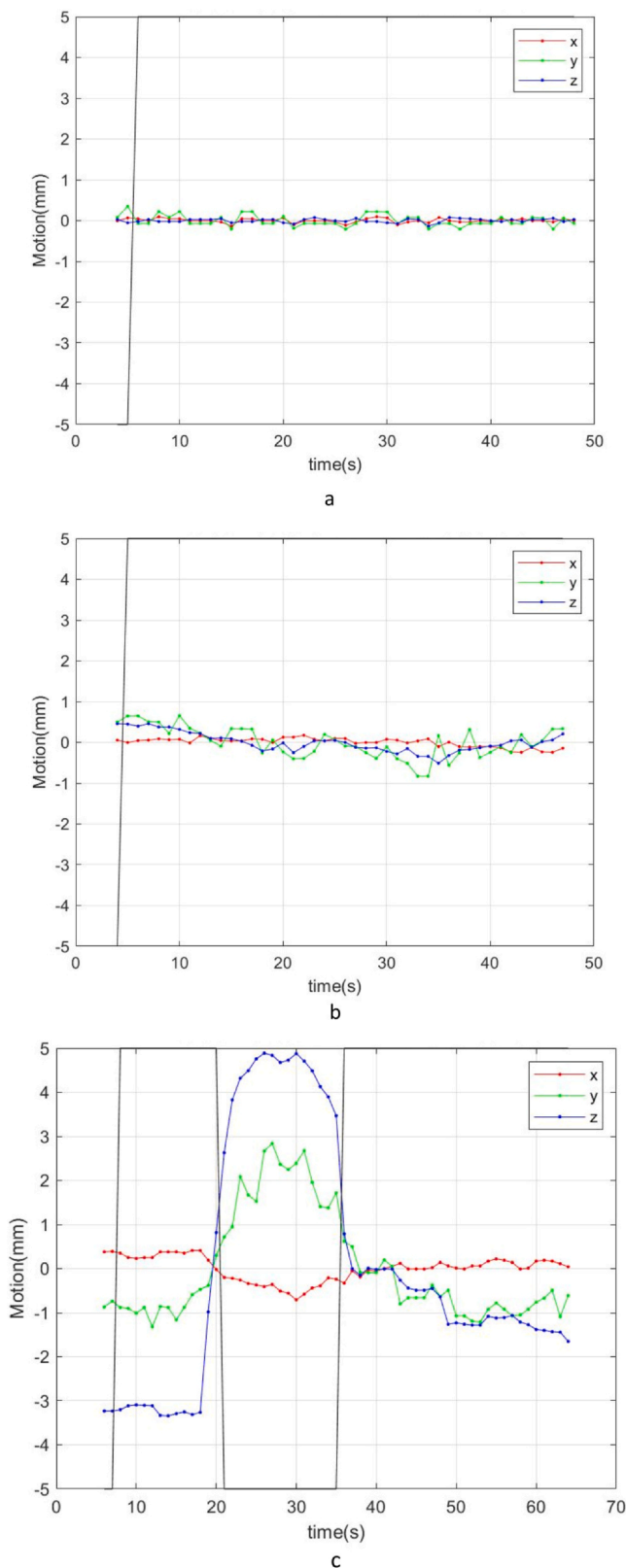


**Figure 5.** (A) Fiducial marker motion ( $< 0.5$  mm) and gating signal during field delivery. (B) Fiducial marker motion ( $< 1$  mm) and gating signal during field delivery. (C) Real-time gated proton therapy turns off the beam when fiducial marker moves out of tolerance.

**Conclusion**

In this paper, we introduce and commission RGPT with the Hitachi proton system combined with fiducial marker evaluation through end-to-end testing. This RGPT uniquely utilized a matching score to evaluate and predict potential delivery issues by triggering the safety interlock. The matching score was fully investigated through the commissioning and clinic procedure setup. The plan delivery efficiency and dose accuracy heavily depended on the setup parameters of the RGPT system. It was then important to establish the proper clinical workflow with sufficient documentation for training and implementation with detailed instructions for therapists provided.

We have successfully treated patients with prostate cancer using RGPT at our proton center for proof of principle, which has improved patient treatment in situations where intrafraction motion was greater than expected. With continued data collection regarding intrafraction shifts, we can further improve our current proton planning techniques, decrease patient daily setup uncertainty, and improve the quality of our patient care. We plan to apply RGPT to different tumor sites using this defined end-to-end evaluation process.

**Funding**

None.

**Author contribution**

Hao Chen: Conceptualization, Data curation, Formal analysis, Investigation, Methodology, Project administration, Resources, Software, Validation, Visualization, Writing- Original draft, Writing-Review and editing. Emile Gogineni: Data curation, Formal analysis, Methodology, Writing- review and editing. Yilin Cao: Data curation, Writing- original draft, Writing- review and editing. John Wong: Conceptualization, Funding acquisition, Investigation, Methodology, Project administration, Supervision, Writing- Review and editing. Curtiland Deville: Conceptualization, Data curation, Funding acquisition, Project administration, Supervision, Writing- review and editing. Heng Li: Conceptualization, Funding acquisition, Investigation, Methodology, Project administration, Supervision, Writing - Original draft, Writing- Review, and editing.

**Data Availability Statement**

The authors confirm that the data supporting the findings of this study are available within the article and its Supplementary Materials. Raw measurement data were generated at Johns Hopkins University. Derived data supporting this article are available from the corresponding author (HC) on request.

**Declaration of Conflicts of Interest**

The authors declare that they have no known competing financial interests or personal relationships that could have appeared to influence the work reported in this paper.

**Acknowledgments**

This work was previously presented at the Annual Conference of the Particle Therapy Cooperative Group (PTCOG60) June 27, 2022 to July 2, 2022, Miami, FL, USA.

## Appendix A. Supplementary material

Supplementary material associated with this article can be found in the online version at [doi:10.1016/j.ijpt.2024.01.001](https://doi.org/10.1016/j.ijpt.2024.01.001).

## References

- Liu C, Sio TT, Deng W, et al. Small-spot intensity-modulated proton therapy and volumetric-modulated arc therapies for patients with locally advanced non-small-cell lung cancer: a dosimetric comparative study. *J Appl Clin Med Phys*. 2018;19(6):140–148. <https://doi.org/10.1002/acm2.12459> Epub 2018 Oct 17. PMID: 30328674; PMCID: PMC6236833.
- Shiraishi Y, Xu C, Yang J, Komaki R, Lin SH. Dosimetric comparison to the heart and cardiac substructure in a large cohort of esophageal cancer patients treated with proton beam therapy or Intensity-modulated radiation therapy. *Radiother Oncol*. 2017;125:48–54.
- Li H, Dong L, Bert C, et al. AAPM Task Group Report 290: respiratory motion management for particle therapy. *Med Phys*. 2022;49:e50–e81.
- Mageras GS, Yorke E. Deep inspiration breath hold and respiratory gating strategies for reducing organ motion in radiation treatment. *Semin Radiat Oncol*. 2004;14(1):65–75. <https://doi.org/10.1053/j.semradonc.2003.10.009> PMID: 14752734.
- Hong TS, DeLaney TF, Mamon HJ, et al. A prospective feasibility study of respiratory-gated proton beam therapy for liver tumors. *Pract Radiat Oncol*. 2014;4(5):316–322. <https://doi.org/10.1016/j.prro.2013.10.002> Epub 2013 Nov 22. PMID: 25194100; PMCID: PMC4327929.
- Lu HM, Brett R, Sharp G, et al. A respiratory-gated treatment system for proton therapy. *Med Phys*. 2007;34(8):3273–3278. <https://doi.org/10.1118/1.2756602> PMID: 17879790.
- Gelover E, Deisher AJ, Herman MG, Johnson JE, Kruse JJ, Tryggestad EJ. Clinical implementation of respiratory-gated spot-scanning proton therapy: an efficiency analysis of active motion management. *J Appl Clin Med Phys*. 2019;20(5):99–108. <https://doi.org/10.1002/acm2.12584> Epub 2019 Apr 10. PMID: 30972922; PMCID: PMC6523004.
- Pallotta S, Vanzi E, Simontacchi G, et al. Surface imaging, portal imaging, and skin marker set-up vs. CBCT for radiotherapy of the thorax and pelvis. *Strahlenther Onkol*. 2015;191(9):726–733. <https://doi.org/10.1007/s00066-015-0861-z> Epub 2015 Jun 19. PMID: 26087908.
- Shimizu S, Miyamoto N, Matsuura T, et al. A proton beam therapy system dedicated to spot-scanning increases accuracy with moving tumors by real-time imaging and gating and reduces equipment size. *PLoS One*. 2014;9(4):e94971.
- Nishioka K, Hashimoto T, Mori T, et al. A single-institution prospective study to evaluate the safety and efficacy of real-time-image gated spot-scanning proton therapy (RGPT) for prostate cancer. *Int J Radiat Oncol Biol Phys*. 2022;114(3):e235. <https://doi.org/10.1016/j.ijrobp.2022.07.1198>
- Hill KD, Mann SD, Carboni MP, et al. Variability in radiation dose and image quality: a comparison across fluoroscopy-system vendors, generations of equipment and institutions. *Catheter Cardiovasc Interv*. 2018;92(7):E471–E477. <https://doi.org/10.1002/ccd.27793> Epub 2018 Sep 12. PMID: 30208245; PMCID: PMC6294676.
- Yoshimura T, Shimizu S, Hashimoto T, et al. Analysis of treatment process time for real-time-image gated-spot-scanning proton-beam therapy (RGPT) system. *J Appl Clin Med Phys*. 2020;21:38–49. <https://doi.org/10.1002/acm2.12804>
- Yoshimura T, Shimizu S, Hashimoto T, et al. Quantitative analysis of treatments using real-time image gated spot-scanning with synchrotron-based proton beam therapy system log data. *J Appl Clin Med Phys*. 2020;21:10–19. <https://doi.org/10.1002/acm2.13029>
- Cao Y, Chen H, Gogineni E, Li H, Deville Jr C. Initial experience with real-time gated proton therapy (RGPT) in the definitive treatment of prostate cancer. *Int J Radiat Oncol Biol Phys*. 2022;114(3):e542–e543.